# CHARACTERIZATION OF FLOODED AREAS IN THE 2008 MYANMAR CYCLONE USING ALOS/PALSAR DATA AND DEM

**Keita KATO[1], Fumio YAMAZAKI[2]**

[1]Graduate student, [2]Professor
Department of Urban Environment Systems, Chiba University
1-33 Yayoicho, Inage-ku, Chiba 263-8522, Japan
Tel: (81)-43-290-3528 Fax: (81)-43-290-3558
E-mail: keitakato@graduate.chiba-u.jp, yamazaki@tu.chiba-u.ac.jp

**KEY WORDS:** ALOS/PALSAR, Storm surge, Flooded area, Cyclone Nargis, Supervised classification, Morphological method.

**ABSTRACT:** Detection of flooded areas after the cyclone Nargis, which hit the coast of Myanmar in early May, 2008, is carried out using ALOS/PALSAR data. The region was more severely affected by storm surge caused by the cyclone than strong wind. Using ALOS/PALSAR images with 6.25m resolution, acquired before and after the disaster, the changes of backscattering echo are investigated. The backscattering echo of PALSAR shows the surface condition of the ground and water. Thus the images are used to detect the areas flooded by the storm surge. For this detection, supervised classification and a morphological-filter method are employed. The land-cover of the classified areas is confirmed by a pre-event Terra/ASTER image. The result of this study is further compared with the disaster map developed by UNOSAT and the accuracy of the proposed method is examined.

## 1. INTRODUCTION

It is very important to grasp the extent of damage at an early time when a natural disaster strikes. In this objective, remote sensing technology is quite useful because it can capture the spatial information quickly and widely. Remote sensing is expected to serve efficiently to provide the information of natural disasters which occur in any part of the world, including the areas difficult to access.

There are a number of studies to detect flooded areas or damages caused by disasters using satellite images. Soo et al. (2004) conducted automated flood detection and mapping using Aqua/MODIS images. MODIS data is thought to be effective because it is low-cost and has ample opportunity to capture flooded areas. Wang et al. (2002) studied the method for mapping flood extent in a coastal flood plain using Landsat TM and DEM (Digital Elevation Model). Since these studies employed optical sensor data, the quality of captured imagery strongly depends on the weather condition.

PALSAR (Phased Array type L-band SAR) sensor, onboard the Japanese satellite ALOS (Advanced Land Observing Satellite), has been observing all over the world. The satellite was successfully launched on 24 January, 2006. PALSAR is an active microwave sensor and is capable of all-weather observation, regardless of day and night. PALSAR data is expected to be used for detecting surface deformation caused by human activities and earthquakes, sea ice monitoring, making DEM, and so on. In order to detect flooded areas, SAR images were also employed by Chunming (2005) and Sohn (2005). UNOSAT showed many disaster maps using SAR images. Matsuoka (2006) detected affected areas by various natural disasters using ALOS/PALSAR imagery.

In this paper, detection of flooded areas using the PALSAR images acquired before and after the cyclone Nargis, which hit Myanmar in the early May 2008, is conducted. The extracted flooded areas are compared with the map illustrated by UNOSAT using MODIS images. To achieve the objective, land cover classification of the study area is performed using Terra/ASTER imagery.

## 2. CYCLONE IN MYANMAR AND SAR IMAGES OF AFFECTED AREA

Between 1st and 3rd of May, 2008, a large cyclone “Nargis” hit the south coast of Myanmar, and brought a catastrophic damage to this area. About 138,000 people were killed, and about 800,000 buildings were collapsed. Especially, the areas along the coast and near the rivers were suffered from serious damages due to storm surge.

After the cyclone passed, ALOS/PALSAR captured an L-band backscatter intensity image of the affected area on 6th May. This image is the fastest captured image after the disaster. It is in the fine mode with 6.25m resolution. The area is located in 160 km southwest from Yangon, the capital city of Myanmar. This area was also captured by PALSAR before the disaster (March 26, 2008) in the fine mode. This study uses these two images (Figure1), which captured the place before and after the event. Although these two images are captured in different paths, the backscatter intensity of water and ground is similar to compare. The backscattering echo decreases if an area is covered by water. Hence, the flooded areas can be detected comparing the backscattering echo between the two images.

For the SAR intensity data, Lee filter with 5*5 pixel window size was applied to reduce speckle noise. Registration was then carried out to these pre- and post- event images. The extraction of flooded areas was conducted using the co-registered two intensity images.

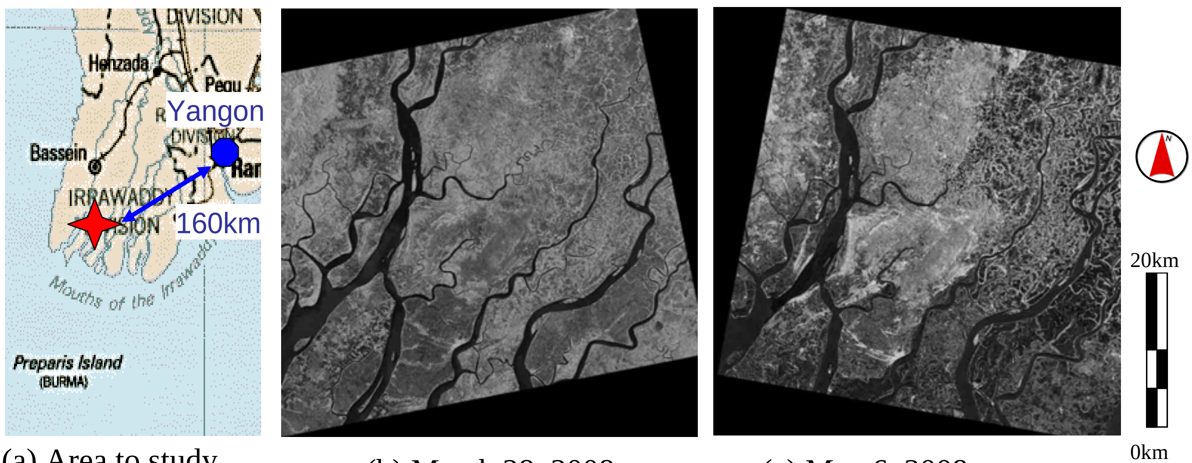


(a) Area to study (b) March 28, 2008 (c) May 6, 2008

Figure 1. PALSAR images of a part of the flooded area in Myanmar

## 3. LAND COVER CLASSIFICATION OF SAR INTENSITY IMAGES

In this study, the flooded areas by storm surge were extracted by a pixel-based supervised classification, using the pre-event and post-event PALSAR intensity images. It is based on the maximum likelihood method. Both the pre-event and post-event images are used in the classification. To obtain a visible image, blue color was assigned to the pre-event SAR intensity image, and red and green colors (yellow color) were assigned to the post-event image. The resultant color composite image is shown in Figure 2 (a). A supervised classification was carried out with four colored areas: *white*, *black*, *blue*, and *yellow*, as training data. Places and histograms of training data are shown in Figure 2 (b), (c). The result of classification is shown in Figure 3.

In this classification, the white and black areas represent the areas with almost no change in backscattering echo between the pre- and post-event images. The blue area indicates a flooded zone because the backscattering echo decreases significantly in the post-event image. On the contrary, the yellow area represents that the backscattering echo increased. The backscatter intensity may increase after flooding because of the seasonal effects, however, the seasonal changes and the differences of weather condition were not taken into account in this study. The yellow color was assumed to be forest areas based on the observation of a pre-event optical image. The black area is thought as permanent water like rivers.

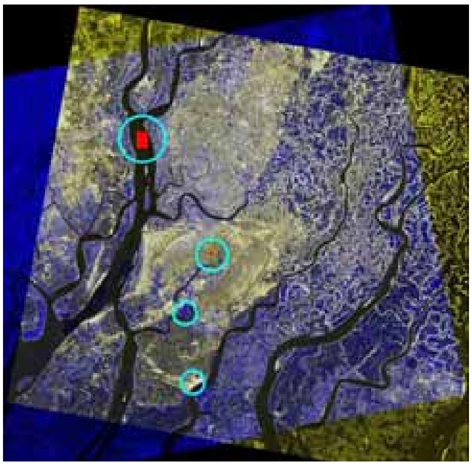

(a) The resultant color composite image

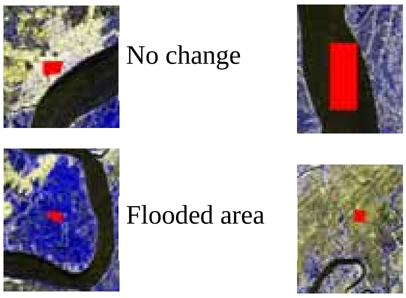


(b) Areas of training data

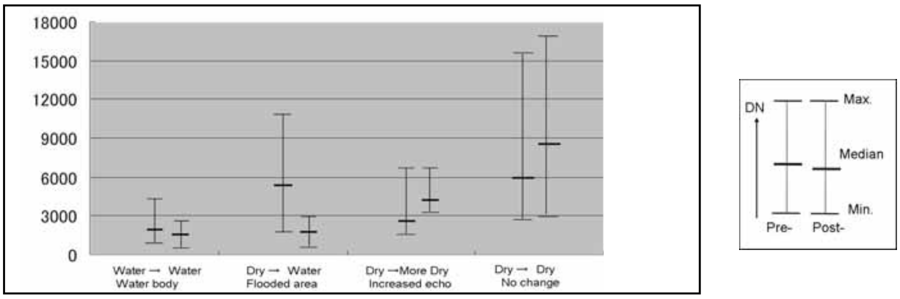


Standard deviation 315 275 1406 379 586 814 2370 1954

(c) Range of DN of each training data

Figure 2. Classification based on the maximum likelihood method

Figure 4 shows the scatter plot of the result of classification. A maximum likelihood classification is conducted based on the DN (Digital Number). Maximum value of DN is 65,535 (=$2^{16}$-1). The resultant DN threshold value of water is about 2,639 for the pre-event image, and about 2,571 for the post-event one. Thus the pixels with DN > about 2,639 in the pre-event image were considered as above water, and the pixels with DN $\leq$ about 2,571 in the post-event image were considered as under water. The areas satisfying these two conditions are considered to be flooded due to the storm surge.

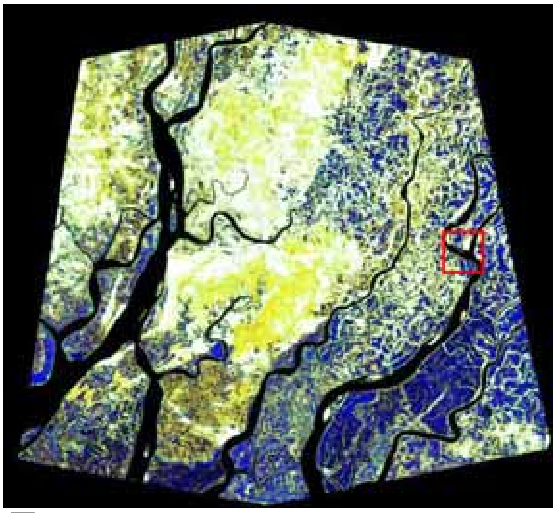

| | | |
|---|---|---|
| ■ | Flooded area | 3,962,383 pixels(20%) |
| ■ | Increased echo | 3,407,724 pixels(18%) |
| □ | No change (High value) | 7,222,358pixels(37%) |
| ■ | Water body (Low value) | 4,818,907pixels(25%) |

Figure 3. Result of classification

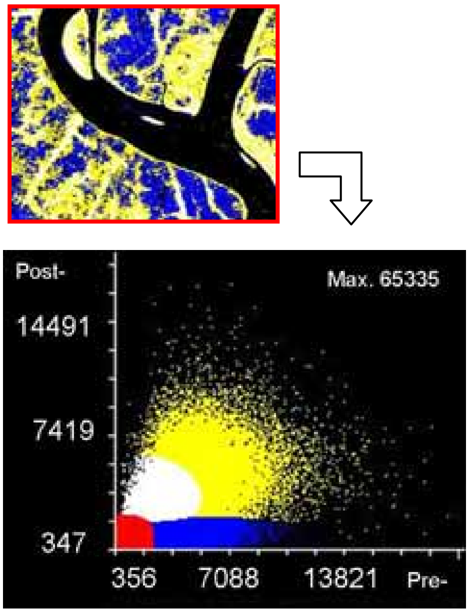


Figure 4. Scatter plot for the four classes by maximum likelihood classification (Red color is water body)

## 4. CHARCTERISTICS OF FLOODED AREAS

Result of supervised classification is further examined using DEM from Shuttle Radar Topography Mission (SRTM) data. Figure 5 is the number of pixels for each elevation. It is seen that the elevation of the flooded area is less than 8m. On the other hand, if the elevation is more than 9m, only the areas with increased echo or no change exist.

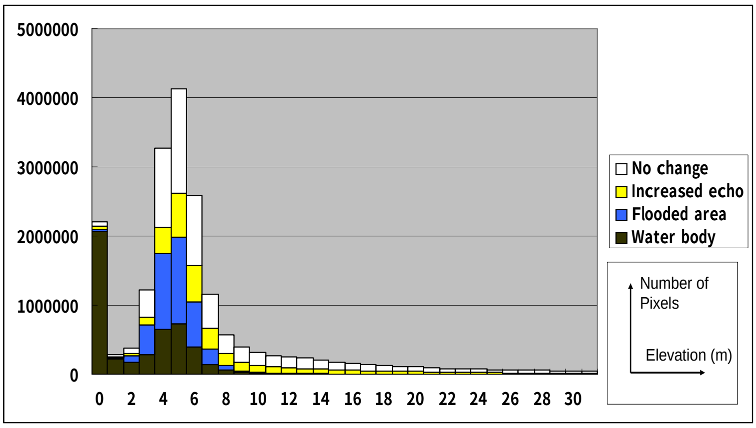


Figure 5. Number of pixels for each elevation

The result from the SAR images was further examined using Terra/ASTER image obtained on March 18, 2007 (Fig. 6) to investigate a detailed pre-event land-cover classification. This information is useful to identify the areas susceptible to be under-water. The ASTER image was employed to classify the areas into three types: water body, field, and forest, by visual inspection. Clouds and shadows were manually removed from the image. The areas with deep red color were visually detected as forests. QuickBird image from Google Earth was also taken into account to identify land covers. Then, the result of maximum likelihood classification of SAR imagery was compared with that of the visual inspection (Table 1). According to the table, 79% of water body is classified correctly. The flooded area detected by the SAR imagery was mainly classified as the fields. The increasing echo areas were mostly located in the forests.

Table 1. Comparison of land-cover classification for the SAR data and the pre-event ASTER image (%)

| | | Land cover for the pre-event ASTER image | | |
|---|---|---|---|---|
| | | Water body | Fields | Forests |
| Result of classification for SAR images | Water body | 79 | 11 | 10 |
| | Flooded area | 4 | 77 | 19 |
| | No change | 1 | 82 | 17 |
| | Increased echo | 2 | 40 | 58 |

Figure 6. False color composite for the pre-event ASTER image

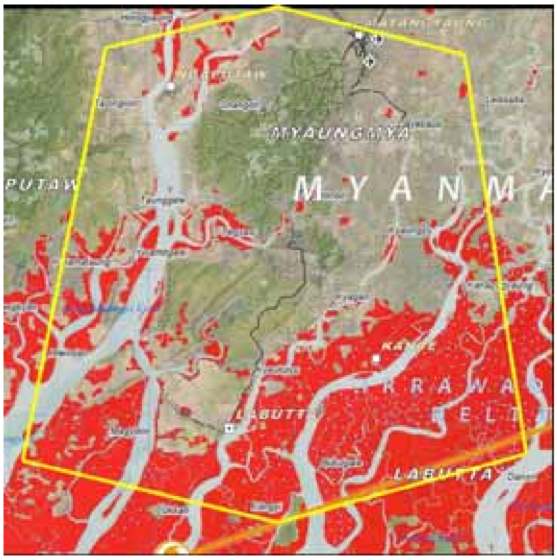


Figure 7. Flooded area map using MODIS constructed by UNOSAT

## 5. COMPARISION WITH DISASTER MAP DEVELOPED BY UNOSAT

Since salt-and-pepper noises were seen in the estimated flooded zone in result of supervised classification, a morphological filter (Vu et al., 2005) was applied to remove the noises and to fill small holes in flooded area. In this method, a 3*3 closing filter was applied twice for the image, and then a 5*5 opening window was applied. Then, small holes and noises were mainly removed.

Detected flooded area by our proposed method is compared with the map of flooded area using MODIS, on board Aqua satellite, drawn by UNOSAT (Fig. 7). MODIS image was captured shortly after the disaster, May 5, 2008. The resolution of MODIS images is 250m. The distribution of estimated flooded areas looks similar between the two results. But, since there is a big difference in their spatial resolution, a detailed comparison is difficult. To obtain a solid conclusion, however, more detailed ground truth data is necessary.

## 6. CONCLUSIONS

Detection of flooded areas after the cyclone Nargis, which hit the coast of Myanmar in early May, 2008, was carried out using the backscattering echo from the pre- and post-event PALSAR images. A supervised classification was carried out for the pre- and post-event SAR intensity composite. The land-cover and elevation of the classified areas were investigated using a pre-event ASTER image and DEM from SRTM. It is found that the elevation of the estimated flooded areas was less than 8m, and the flooded areas were located in the fields. The result of this study was also compared with the disaster map by UNOSAT and the distribution of the flooded areas was agreed in a macro sense. Some additional ground truth data are necessary to discuss more on the accuracy of the present flood estimation.

## ACKNOWLEDGMENTS

ALOS/PALSAR images employed in this study were provided by Japan Aerospace Exploration Agency (JAXA). ASTER images were provided by Global Earth Observation Grid (Geo Grid), National Institute of Advanced Industrial Science and Technology (AIST), Tsukuba, Japan.

## REFERENCES

Chunming H., Huadong G., and Jingjuan L., 2005. Detection of the Flood Boundary in SAR Image Using Texture, *Proceedings of Geoscience and Remote Sensing Symposium 2005*, IEEE International, Volume5, pp 3697- 3699

International Charter, URL: http://www.disasterscharter.org/

Matsuoka, M., Use of ALOS/PALSAR Imagery for Monitoring Areas Damaged due to Recent Natural Disasters, Disaster Forewarning Diagnostic Methods and Management, 2006, *Proceedings of SPIE*, Vol.6412, ID641204, 7p.

Sohn H.G., Song Y.S., and Kim G.H., 2005. Detecting Water Area During Flood Event from SAR Image, *ICCSA 2005*, LNCS 3481, pp. 771 – 780.

Soo L., Liew C., and Kwoh L. K., 2004. Automated Realtime Flood Detection and Mapping Using Terra MODIS, *Proceedings of 25th Asian Conference on Remote Sensing*, pp.222-228.

UNOSAT, URL:http://unosat.web.cern.ch/unosat/freeproducts/Myanmar/Cyclone/UNOSAT Myanmar_MODIS_5May2008_Frood_ Labutta_Township_Lowres_v2.pdf

USGS, URL:http://srtm.usgs.gov/

Vu T. T., Matsuoka M., and Yamazaki F., 2005. Detection and Animation of Damage Using Very High Resolution Satellite Image Following the 2003 Bam, Iran, Earthquake. *Earthquake Spectra*, Vol.21, No. S1, pp. S319-S327.

Wang Y., Colby J. D. and Mulcahy K. A., 2002. An Efficient Method for Mapping Flood Extent in a Coastal Flood Plain Using Landsat TM and DEM data, *International Journal of Remote Sensing*, vol. 23, no. 18, 3681–3696.